Electronic Supplementary Material (ESI) for Journal of Materials Chemistry A.

Supporting Information

Nitrogen-Doped Graphdiyne Nanowalls Stabilized Dendrite-Free Lithium Metal Anodes

Tao Jiang[a†], Ke Chen[b†*], Jingjing Wang[c†], Zhongli Hu[a], Gulian Wang[a], Xu-Dong Chen[c*], Pengfei Sun[a], Qiaobao Zhang[d], Chenglin Yan and Li Zhang[a*]

[a.] *College of Energy, Soochow Institute for Energy and Materials InnovationS, Key Laboratory of Advanced Carbon Materials and Wearable Energy Technologies of Jiangsu Province, Soochow University, Suzhou 215006, China. E-mail: zhangli81@suda.edu.cn*

[b.] *Institute of Micro/Nano Photonic Materials and Applications, School of Physics and Electronics, Henan University, Kaifeng 475004, China. E-mail: kchen@henu.edu.cn*

[c.] *Institute for New Energy Materials and Low Carbon Technologies, School of Materials Science and Engineering, Tianjin University of Technology, Tianjin 300384, China. E-mail: chenxd@email.tjut.edu.cn*

[d.] *Department of Materials Science and Engineering, College of Materials, Xiamen University, Xiamen 361005, Fujian, China*

[†] *These authors contributed equally to this work.*

➢ Supporting Information Notes

Supplementary note 1

Electrochemistry: The nucleation overpotential and Coulombic efficiency was performed on a LAND CT2001A battery testing system. For the Li plating/stripping cycling efficiency measurement, the batteries were first cycled in a potential range of 0-1 V at 50 μA for five cycles to stablize the SEI and remove surface contaminations. 1 mAh·cm^{-2} (or 3 mAh·cm^{-2}, 5 mAh·cm^{-2}) of Li was then deposited onto the working electrodes (GDY and N-GDY) and charged to 0.5 V at various current densities from 1 to 5 mA·cm^{-2} for each cycle. The Coulombic efficiency was calculated based on the ratio of Li stripping to plating. Rate capability of N-GDY electrodes were measured at current densities ranging from 0.5 to 6 mA·cm^{-2} for 1 h in both the stripping/plating processes of each cycle. The long-term cycling stability and voltage hysteresis were investigated through a symmetric Li/Li test, GDY and N-GDY hosts were firstly plated by Li metal with a pre-stored capacity of 2 mAh·cm^{-2} (or 5 mAh·cm^{-2}, 8 mAh·cm^{-2}), then cycled at various current densities with a constant areal capacity of 1 mAh·cm^{-2} (or 3 mAh·cm^{-2}, 5 mAh·cm^{-2}). Electrochemical impedance spectroscopy (EIS) was measured after different electrochemical cycles by applying an alternating voltage of 5 mV over the frequency ranging from 10^{-2} to 10^{5} Hz.

Full cells were constructed with a $LiNi_{0.5}Co_{0.2}Mn_{0.3}O_2$ (NCM) cathode and a N-GDY@Li anode with a pre-stored capacity of of 5 mAh·cm^{-2} (or pure Li metal). The NCM electrodes were punched into circle discs of *ca*. 0.33 cm^2 and the areal mass loading of NCM was ~3 mg cm^{-2}. Cyclic voltammetry (CV) measurements were performed in a potential range of 2.8-4.3 V at a scan rate of 0.1 mV s^{-1}. Galvanostatic charge-discharge cycling tests of N-GDY@Li||NCM and Li||NCM full cells were carried out in a potential range of 2.8-4.3 V at 0.2 C, corresponding to a current density of 0.096 mA·cm^{-2}.

Supplementary note 2

DFT simulations: Density functional theory (DFT) simulations were performed using the Vienna Ab-initio Simulation Package (VASP) package. The generalized gradient approximation (GGA) with the Perdew-Burke-Ernzerhof (PBE) functional was employed to describe the electronic exchange and correlation effects. Uniform G-centered k-points meshes with a resolution of 2π*0.03 $Å^{-1}$ and Methfessel-Paxton electronic smearing were adopted for the integration in the Brillouin zone for geometric optimization. The simulation was run with a cutoff energy of 500 eV throughout the computations. These settings ensure convergence of the total energies to within 1 meV per atom. Structure relaxation proceeded until all forces on atoms are less than 1 meV $Å^{-1}$ and the total stress tensor is within 0.01 GPa of the target value. The adsorption energy (ΔE_{ads}) was estimated by the following formula:

ΔE(ads) = [E(surface+n*Li)-E(surface)-n* E(Li)]/n

where n is the number of adsorbed Li atoms, E(surface+n*Li) is the total energy of the surface adsorbed n Li atoms, E(surface) is the total energy of the Cu (111) or carbon-based surfaces, and E(Li) is the total energy of one Li atom.

➢ Supporting Information Figures

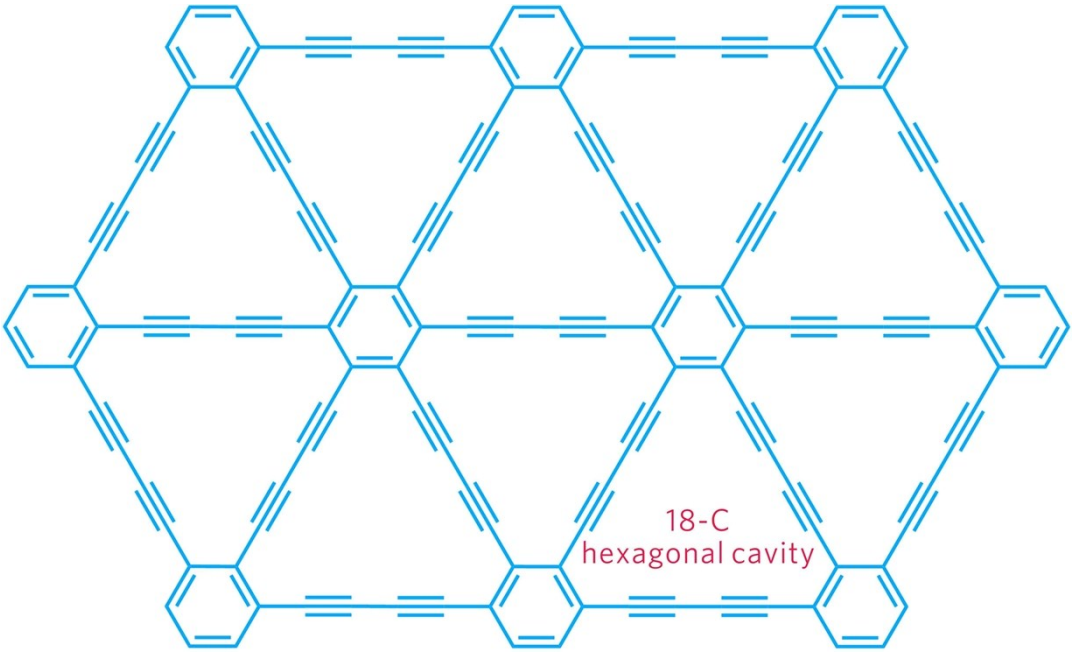

Fig. S1. Schematic structure of a single-layer graphdiyne.

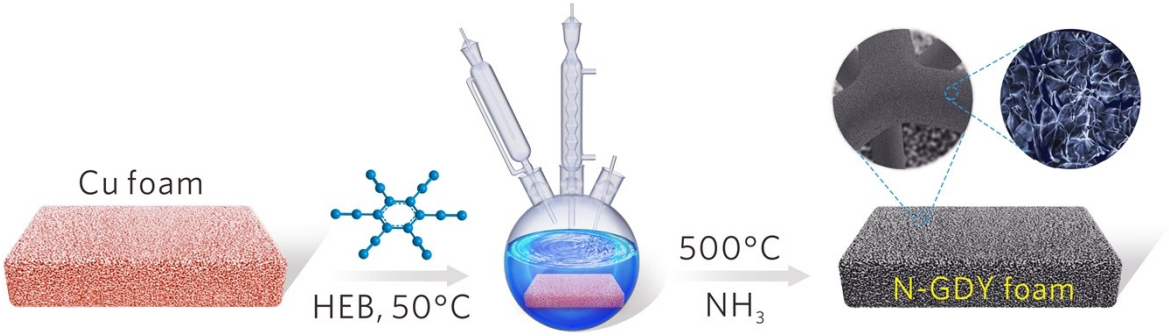

Fig. S2. Schematic of the synthetic procedure of the N-GDY host.

Fig. S3. Digital photographs of the pristine Cu foam, GDY host after the low-temperature wet-chemistry synthesis, and N-GDY host after the thermal nitridation process.

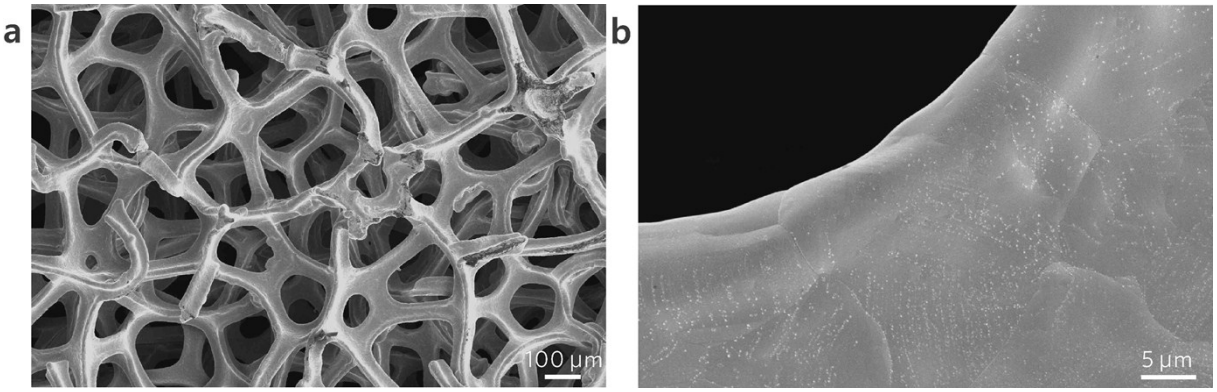

Fig. S4. SEM images of the pristine Cu foam at different magnifications.

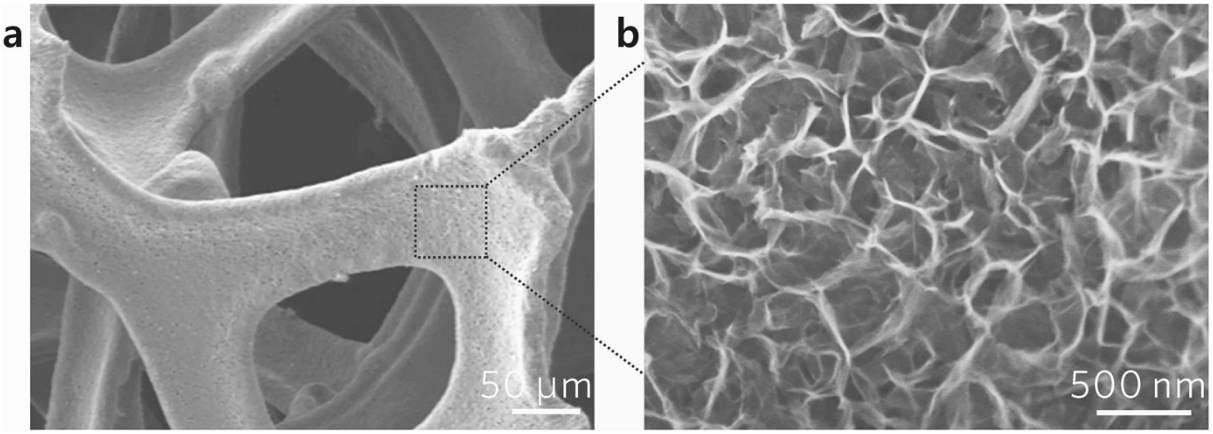

Fig. S5. SEM images of the as-obtained GDY foam at different magnifications.

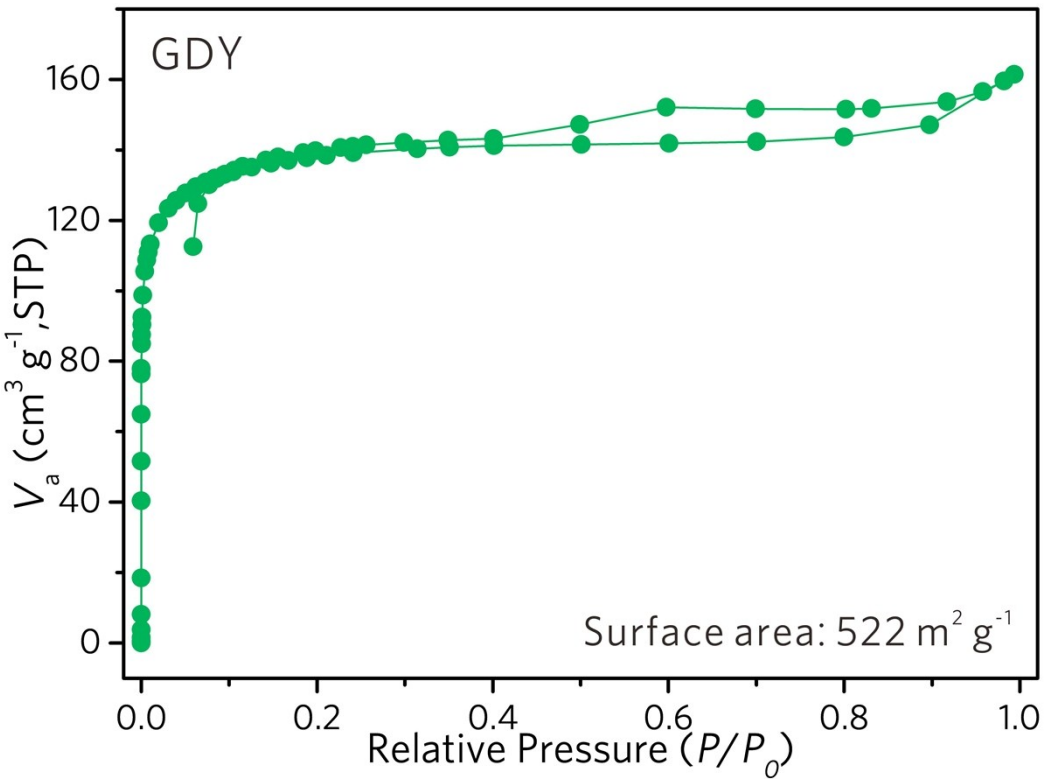

Fig. S6. N_2 adsorption-desorption profiles of N-GDY powders that are stripped from the 3D Cu foam.

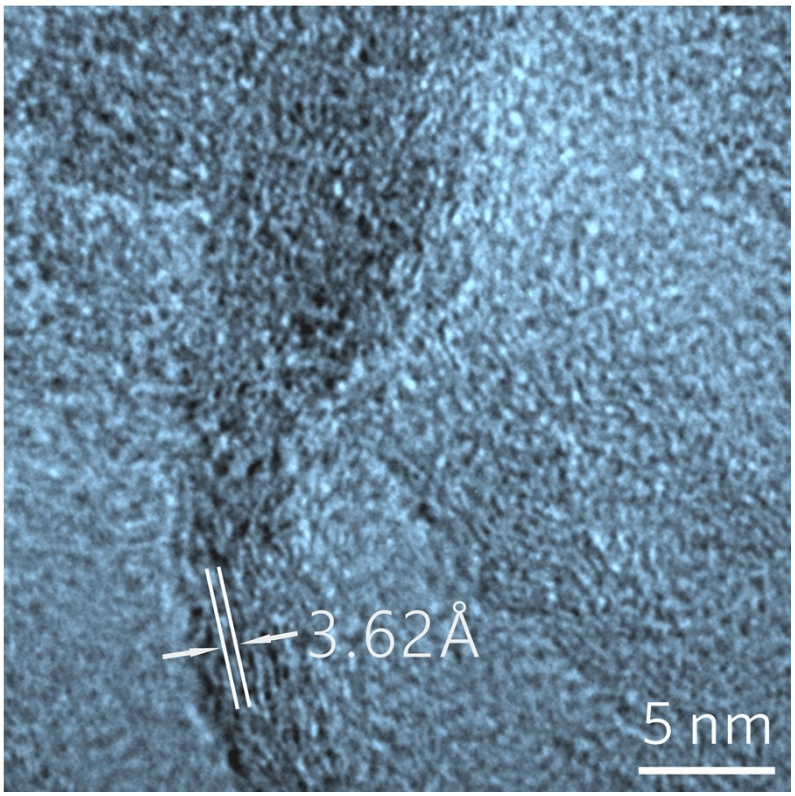

Fig. S7. HRTEM image of the as-obtained N-GDY nanowalls.

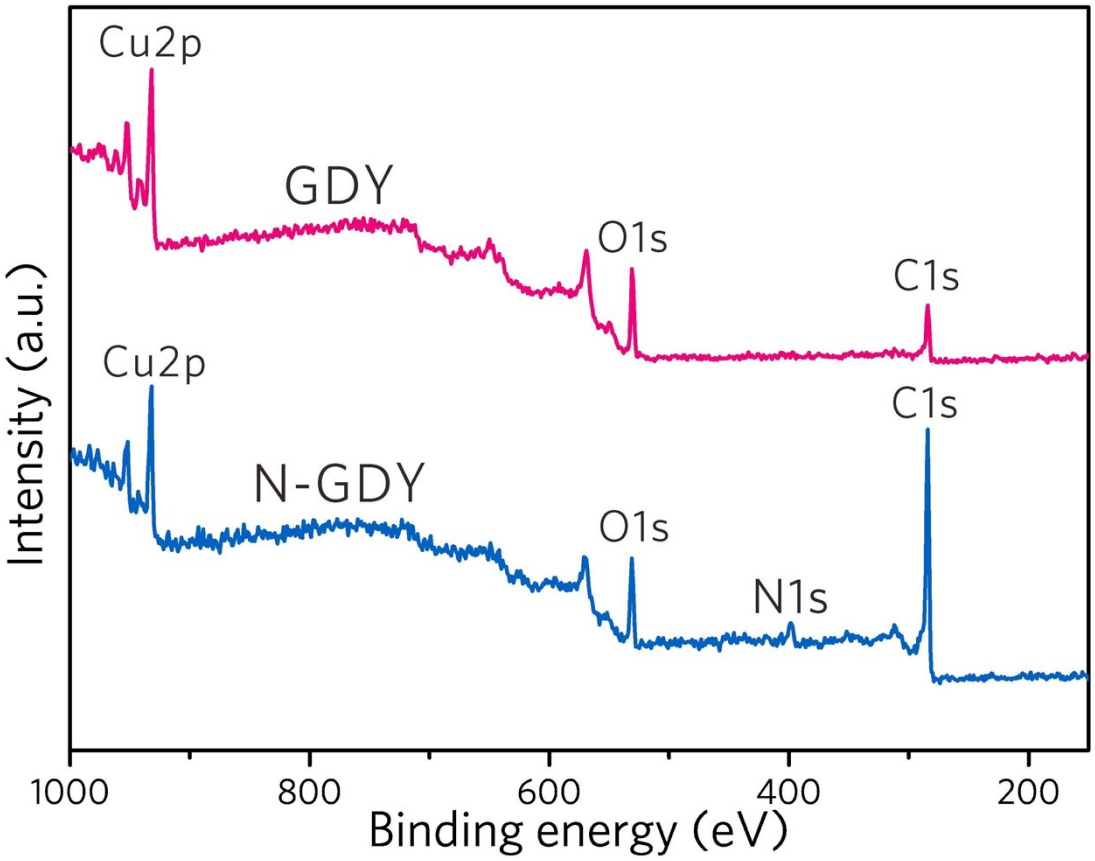

Fig. S8. Full-scan XPS spectra of GDY and N-GDY hosts displaying C, O and N signals.

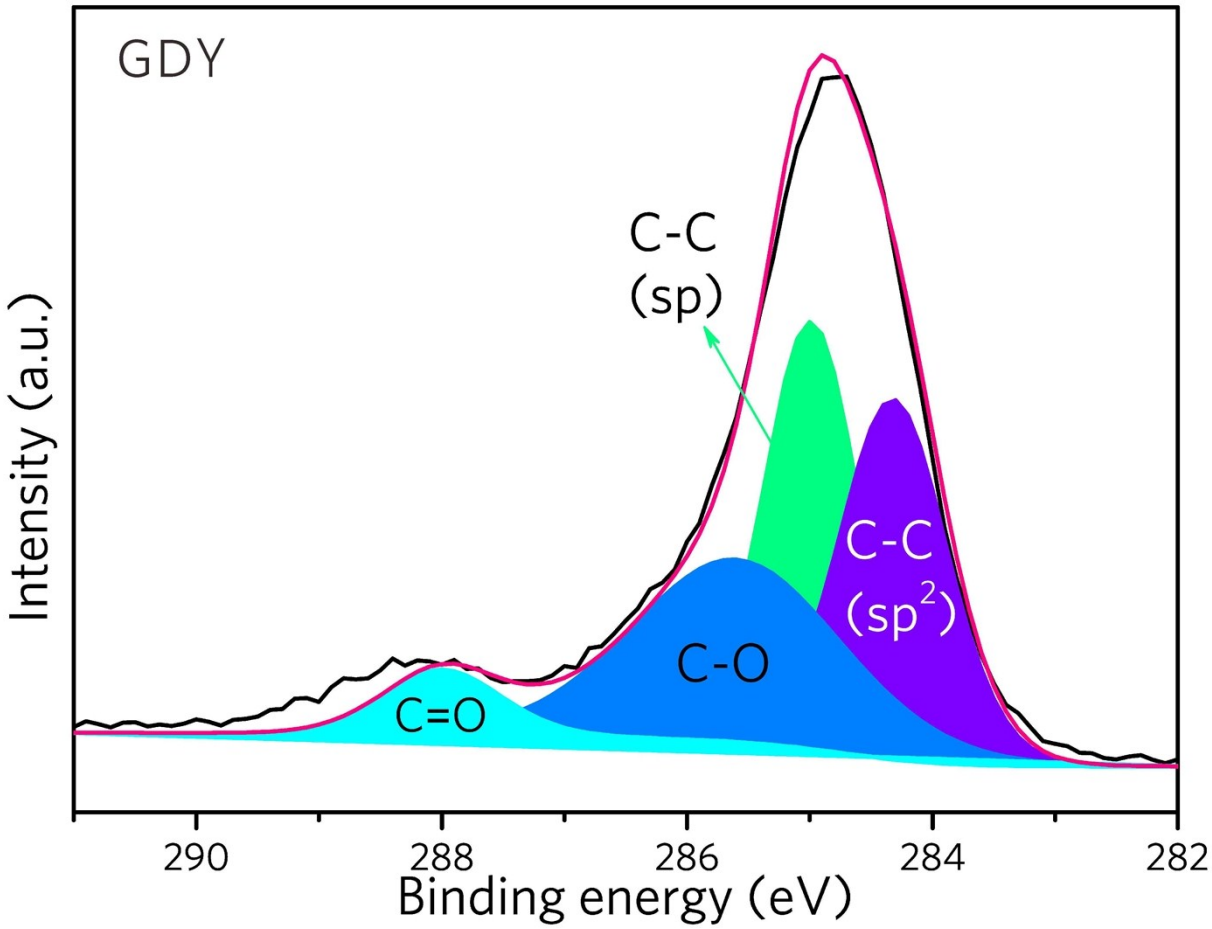

Fig. S9. High-resolution *C 1s* spectrum of the GDY foam.

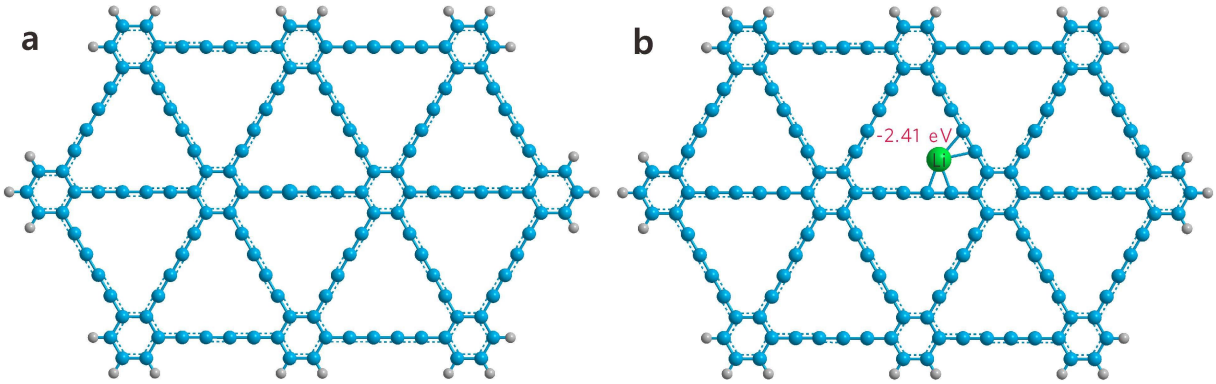

Fig. S10. Optimized models of the Li atom binding to non-doped graphdiyne.

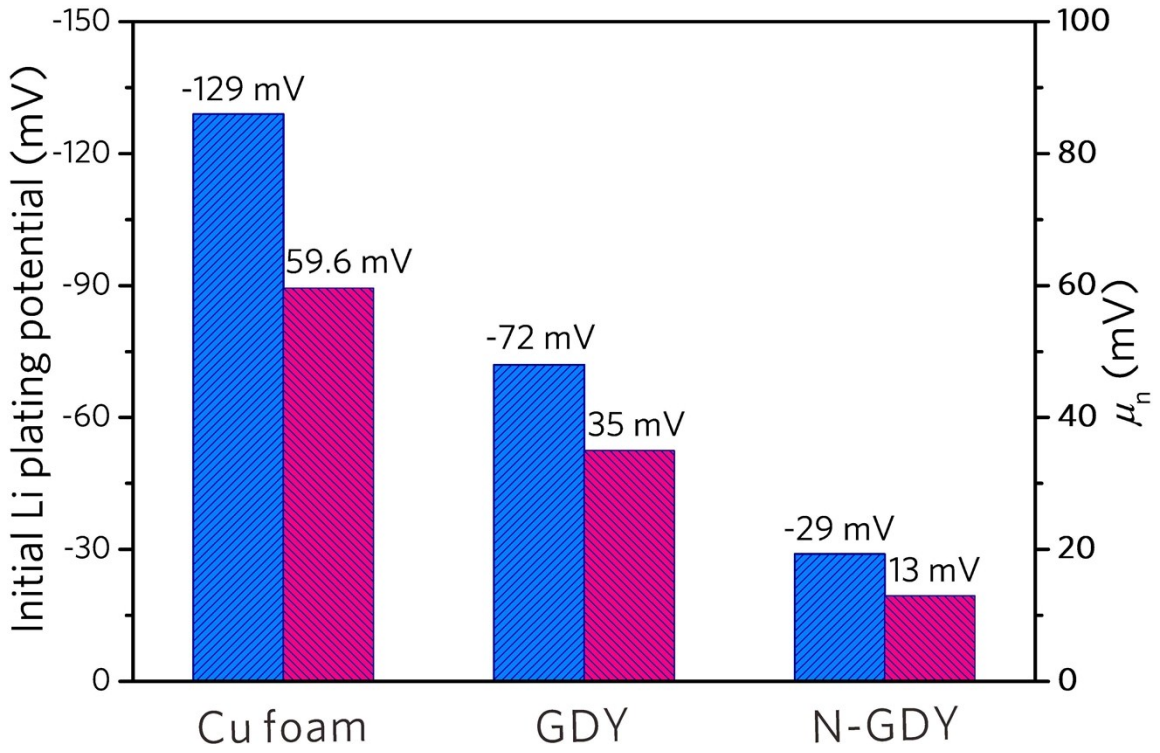

Fig. S11. The initial nucleation potentials and nucleation overpotentials (μ_n) of the Cu foam, Cu@DGY and N-DGY electrodes.

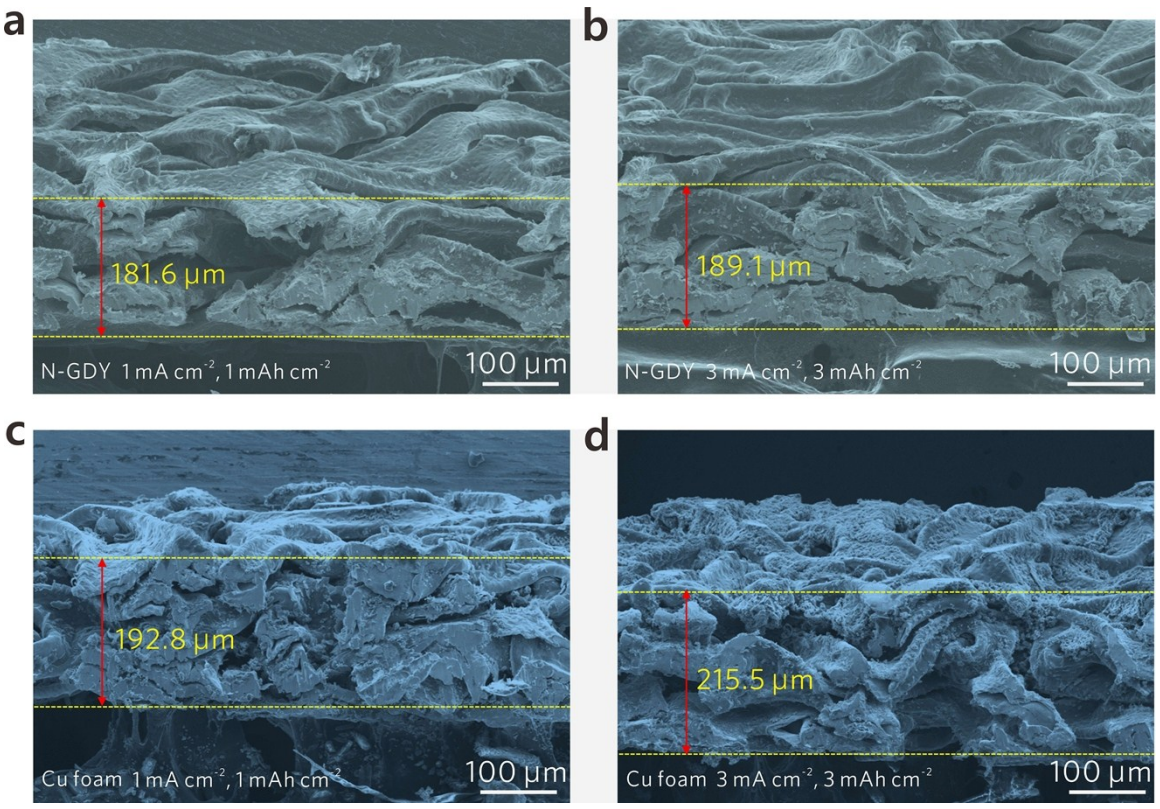

Fig. S12. Cross-section SEM images of a, b) the N-GDY and c, d) Cu foam substrates after depositing Li under two different conditions of 1 mAh·cm^{-2}/1 mA·cm^{-2} and 3 mAh·cm^{-2}/3 mA·cm^{-2} at the same 20th cycle.

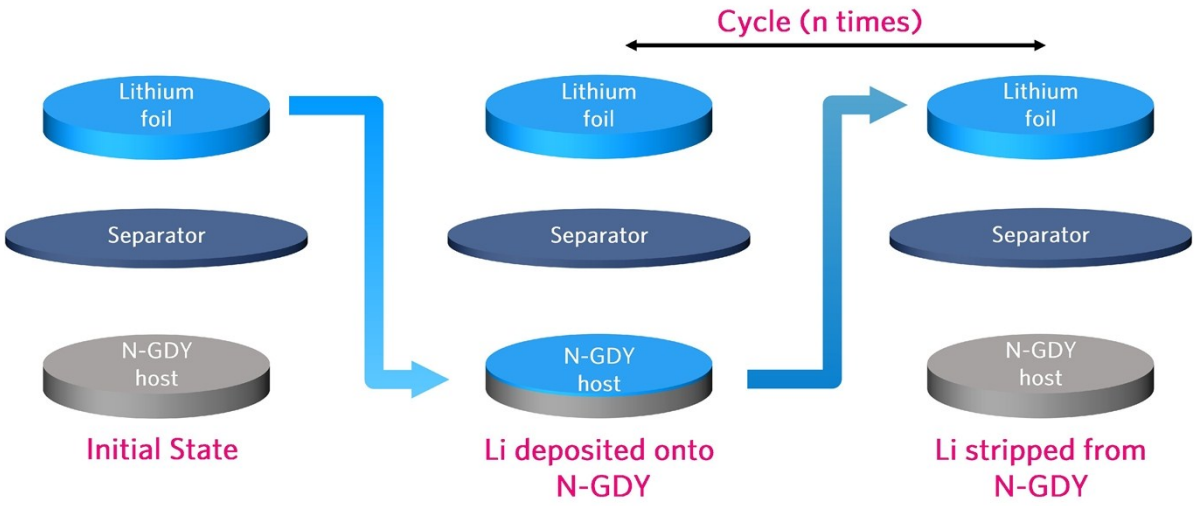

Fig. S13. Schematic diagram of cycling half cells for measurement of the Li plating/ stripping Coulombic efficiency during long-term cycling.

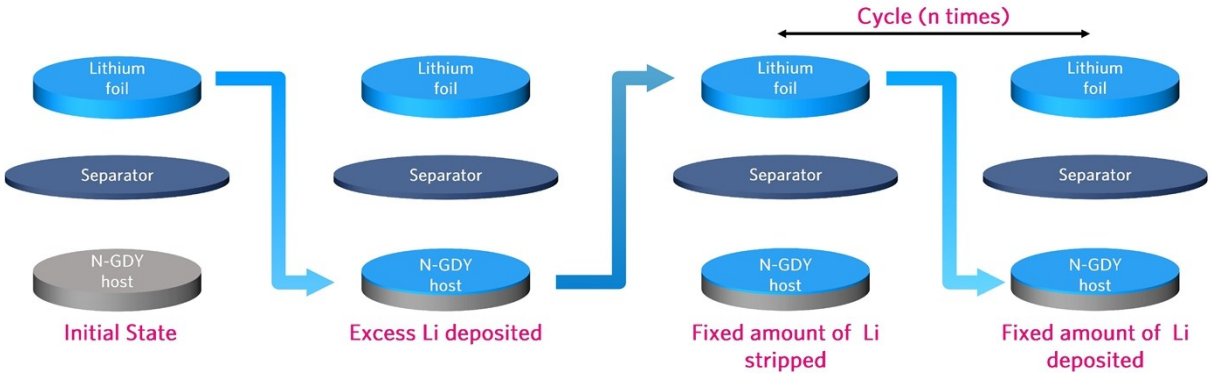

Fig. S14. Schematic diagram of cycling symmetric cells for measurement of the cycling stability and voltage hysteresis during long-term cycling.

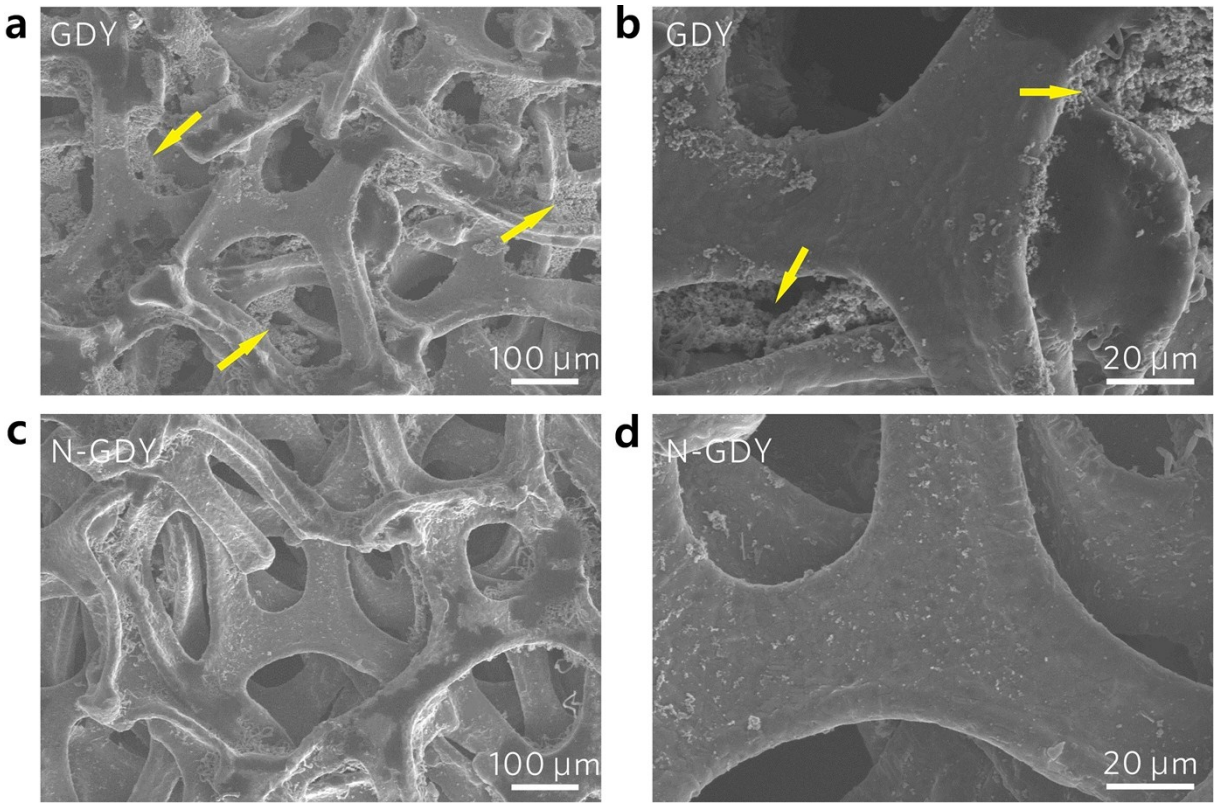

Fig. S15. SEM images of the GDY@Li and N-GDY@Li electrodes after the 25th Li stripping/plating (3 mA·cm^{-2} and 3 mAh·cm^{-2}) in their charged states with a residue of 2 mAh·cm^{-2} Li.

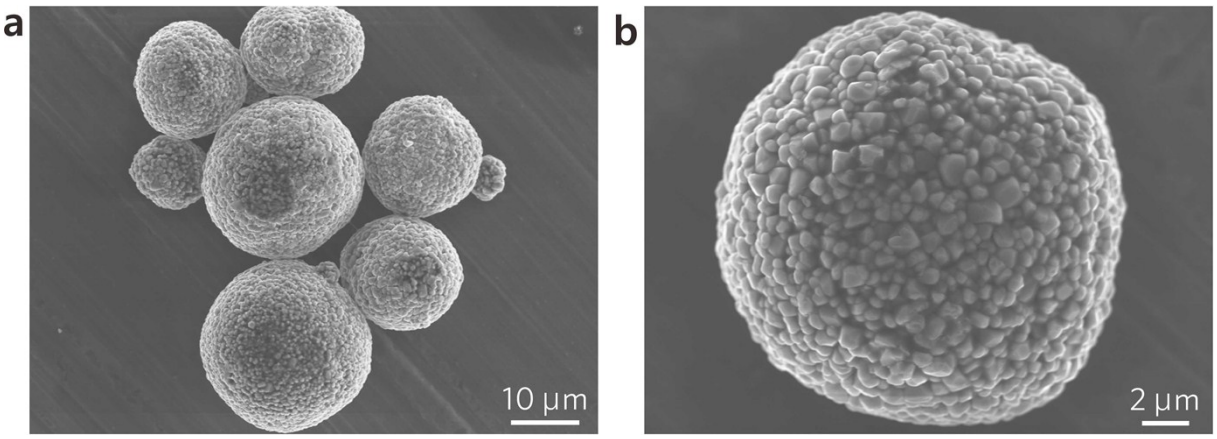

Fig. S16. SEM images of the commercial NCM powders at different magnifications.

➢ Supporting Information Tables

Table S1. The calculated binding energies of Li atom with Cu, VG, un-doped GDY and different functional groups in N-GDY.

	E(surface+n*Li)	*E*(surface)	*E*(Li)	Δ*E*(ads)
Cu	-128.03115268	-125.56868228	-0.07691098	-2.38556
VG	-664.90602816	-661.65694673	-0.07691098	-3.1721705
GDY	-1245.5995159	-1243.1136841	-0.07691098	-2.4089208
N(*α*)	-1244.7034133	-1242.1785241	-0.07691098	-2.4479782
N(*β*)	-1244.2592898	-1241.8330269	-0.07691098	-2.3493519
N(*γ*)	-1244.3618429	-1241.1065557	-0.07691098	-3.1783762
N(*δ*)	-1243.2989976	-1239.6315907	-0.07691098	-3.5904959
N(*ε*)	-1239.9926123	-1238.3202938	-0.07691098	-1.5954075

Table S2. Comparison of the electrochemical performances between the N-GDY hybrid host and other porous Cu and carbon allotropes hosts previously reported.

3D porous matrix host	Current density (mA·cm-2)	Cycling capacity (mAh·cm-2)	Stable cycling numbers	Ref.
N-GDY host	1	1	>720	This work
	5	1	>260	
	1	5	>30	
	3	3	>175	
3D Porous Cu	1	1	~300	1
3D Cu	0.2	0.5	>120	2
3D hollow tubular carbon fiber	1	2	>60	3
3D porous Ni core-shell	3	1	>315	4
Hollow carbon nanospheres	1	1	>75	5
3DNG	0.5	1	~150	6

Graphitized carbon fibers	1	1	>500	7
Nitrogen-doped graphene	1	1	>727	8
G-C_3N_4	1	1	>450	9
Unstacked graphene drum	2	0.1	>800	10
Cu@VG foam	1	1	>160	11
	3	3	>50	

Reference for Table S2

[1] Q. Li, S. Zhu and Y. Lu, *Adv. Funct. Mater.*, 2017, **27**, 1606422.

[2] C. P. Yang, Y. X. Yin, S. F. Zhang, N. W. Li and Y. G. Guo, *Nat. Commun.*, 2015, **6**, 8058.

[3] L. Liu, Y. X. Yin, J. Y. Li, N. W. Li, X. X. Zeng, H. Ye, Y. G. Guo and L. J. Wan, *Joule*, 2017, **1**, 563-575.

[4] L. L. Lu, Y. Zhang, Z. Pan, H. B. Yao, F. Zhou and S. H. Yu, *Energy Storage Mater.*, 2017, **9**, 31-38.

[5] G. Zheng, S. W. Lee, Z. Liang, H. W. Lee, K. Yan, H. Yao, H. Wang, W. Li, S. Chu and Y. Cui, *Nat. Nanotechnol.*, 2014, **9**, 618-623.

[6] R. Zhang, S. Wen, N. Wang, K. Qin, E. Liu, C. Shi and N. Zhao, *Adv. Energy Mater.*, 2018, **8**, 1800914.

[7] T. T. Zuo, X. W. Wu, C. P. Yang, Y.X. Yin, H. Ye, N. W. Li and Y. G. Guo, *Adv. Mater.*, 2017, **29**, 1700389.

[8] G. Huang, J. Han, F. Zhang, Z. Wang, H. Kashani, K. Watanabe and M. Chen, *Adv. Mater.*, 2019, **31**, 1805334.

[9] Z. Lu, Q. Liang, B. Wang, Y. Tao, Y. Zhao, W. Lv, D. Liu, C. Zhang, Z. Weng, J. Liang, H. Li and Q. H. Yang, *Adv. Energy Mater.*, 2019, **9**, 1803186.

[10] R. Zhang, X. B. Cheng, C. Z. Zhao, H. J. Peng, J. L. Shi, J. Q. Huang, J. Wang, F. Wei and Q. Zhang, *Adv. Mater.*, 2016, **28**, 2155-2162.

[11] Z. Hu, Z. Li, Z. Xia, T. Jiang, G. Wang, J. Sun, P. Sun, C. Yan and L. Zhang, *Energy Storage Mater.*, 2019, https://doi.org/10.1016/j.ensm.2018.12.020.